Line strengths of QED-sensitive forbidden transitions in B-, Al-, F- and Cl-like ions

M. Bilal,[1,2,*] A. V. Volotka,[1] R. Beerwerth,[1,2] and S. Fritzsche[1,2]

[1]*Helmholtz-Institut Jena, Fröbelstieg 3, D-07743 Jena, Germany*
[2]*Theoretisch-Physikalisches Institut, Friedrich-Schiller-Universität Jena, Max-Wien-Platz 1, D-07743 Jena, Germany*

The magnetic dipole ($M1$) line strength between the fine-structure levels of the ground configurations in B-, F-, Al-, and Cl-like ions are calculated for the four elements argon, iron, molybdenum, and tungsten. Systematically enlarged multiconfiguration Dirac-Hartree-Fock (MCDHF) wave functions are employed to account for the interelectronic interaction with the Breit interaction included in first-order perturbation theory. The QED corrections are evaluated to all orders in αZ utilizing an effective potential approach. The calculated line strengths are compared with the results of other theories. The $M1$ transition rates are reported using accurate energies from the literature. Moreover, the lifetimes in the range of millisecond to picosecond are predicted including the contributions from the transition rate due to the $E2$ transition channel. The discrepancies of the predicted rates from those available from the literature are discussed and a benchmark data set of theoretical lifetimes is provided to support future experiments.

I. INTRODUCTION

Transition energies and transition rates are two fundamental properties of atomic states. Therefore, a detailed analysis and comparison of theoretical predictions with experimental observations may provide crucial insight into our basic understanding of the atomic structure. For level energies, there exists a number of cases where very high accuracy has been achieved from both theory and experiment, and has helped make QED and many-body relativistic effects visible. For example, QED has been tested at the level of 7.2% for the $M1$ transition energy between fine-structure levels of the ground configuration in B-like Ar [1–4]. For the transition rates and line strengths, in contrast, the accuracy level is often not yet sufficient to test QED and many-body relativistic effects. This is partially due to theory and partially due to experiment. We know that transition rates depend on higher power of transition energy and nondiagonal matrix elements of the multipolar electromagnetic operators. In contrast to transition energies, there is no variational principle available that defines a minimum condition for the optimization of nondiagonal matrix elements. For this reason, the many-body relativistic effects are more difficult to capture. While the experimental accuracy is typically 2% and higher due to systematic and statistical errors [5–10], this has been found insufficient to explore relativistic and QED effects,; for details, see the reviews [11,12]. However, there are two remarkable exceptions where an accuracy of the order of 0.1% is claimed by efficiently controlling the systematic and statistical errors. Both of these lifetime measurements were performed at the Heidelberg electron beam ion trap (HD-EBIT). The measured lifetime is reported as 9.573(4)(5)(stat/syst) ms for the $2s^2 2p\, ^2P_{3/2}$ level in B-like Ar [13] and 16.726(+20/ − 10) ms for the $3s^2 3p\, ^2P_{3/2}$ level in Al-like Fe [14]. Both of these levels decay dominantly via a magnetic dipole ($M1$) transition between the fine-structure levels of the ground configuration.

In the case of an $M1$ transition between the fine-structure levels of the same configuration the nondiagonal matrix element, i.e., the line strength, is less sensitive than for $E1$ allowed transitions. This is because in the nonrelativistic limit, the $M1$ line strength is insensitive to the description of the many-electron wave functions. In other words, (almost) all correlation corrections are of relativistic origin and, therefore, suppressed by a factor αZ (Z is the nuclear charge). For such transitions the line strengths are especially sensitive to the QED contributions. For instance, the leading QED effect of an order α, the so-called electron anomalous magnetic moment (EAMM) correction, contributes 0.46% [15]. Therefore, such $M1$ transition rates can be calculated very precisely and may be used as a benchmark for comparison with the experiment.

During recent years, various *ab initio* calculations have been reported for the $M1$ line strength between the $2s^2 2p\, ^2P_{3/2} - {}^2P_{1/2}$ levels in B-like ions [15–20] and $3s^2 3p\, ^2P_{3/2} - {}^2P_{1/2}$ in Al-like ions [21,22]. In particular, the line strength of the $2s^2 2p\, ^2P_{3/2} - {}^2P_{1/2}$ transition in B-like Ar has been evaluated with a relative uncertainty of only 10^{-5} [15]. However, all these calculated line strengths combined with experimental transition energies tend to predict shorter lifetimes than measured experimentally [13,14]. In fact, the deviation between theory and experiment is of the order of the EAMM, which led to a speculation about the correctness of the inclusion of the EAMM into the transition amplitude. Let us note here that such high-precision measurements are available only from the HD-EBIT in the millisecond range. In the future, however, precise experiments for various lifetime and transition energy domains and by different techniques will hopefully solve the present discrepancy. Therefore, there is strong need for a theoretical analysis of these systems where relativistic correlations and the QED contributions can be quantified as a benchmark principle for these experiments.

We here present a detailed study for the line strengths of QED-sensitive forbidden transitions between the fine-structure

*Corresponding author: moazzam.bilal@uni-jena.de

levels of the ground configurations in B-, Al-, F-, and Cl-like ions. The ground configurations of B-like and Al-like ions have a valence p electron in the L shell and M shell, respectively. These configurations are also quite similar to the ground configurations of F-like and Cl-like ions but with a p-shell vacancy in the L shell and M shell, respectively. The major difference between the two systems of ions is the flip of fine-structure levels where the excited ^2P ground-state levels dominantly decay through an $M1$ transition. We will combine our accurate line strengths with accurate experimental or theoretical transition energies and predict lifetimes in the millisecond to picosecond range.

The rest of the paper is structured as follows. A short description of the underlying theory and our calculations are described in Sec. II. In Sec. III, we present a detailed comparison of our calculated line strengths with other theories. Here we add contributions from the $E2$ channel and the $M1$ channel. From the total transition rates we predict the lifetimes and compare with available experiments. Finally, our main findings are summarized in Sec. IV. Atomic units ($\hbar = m = e = 1$) are used throughout the paper.

II. THEORY AND CALCULATIONS

A. Theory—Basic formulas

The magnetic dipole transition probability from an upper state i to a lower state f is expressed in terms of the line strength as

$$W = \frac{4}{3} \frac{\omega^3}{c^3} \mu_0^2 \frac{S}{2J_i + 1}, \tag{1}$$

where μ_0 denotes the Bohr magneton, c the speed of light, $\omega = E_i - E_f$ the transition energy, and where the line strength is

$$S = \frac{18c^4}{\omega^2} |\langle \Psi_f \parallel \mathbf{T} \parallel \Psi_i \rangle|^2. \tag{2}$$

$\mathbf{T}$ is the $M1$ transition operator given as

$$\mathbf{T} = \frac{1}{\sqrt{2}} j_1(\omega r/c) \frac{[\boldsymbol{\alpha} \times \mathbf{r}]}{r} = \frac{\sqrt{2}}{r} j_1(\omega r/c)\boldsymbol{\mu}. \tag{3}$$

Here $\boldsymbol{\mu} = -[\mathbf{r} \times \boldsymbol{\alpha}]/2$ is the relativistic magnetic moment operator, $\boldsymbol{\alpha}$ is the Dirac matrix, and j_1 is the spherical Bessel function.

In the nonrelativistic limit the expansion of $j_1(\omega r/c)$ can be restricted to the first term, and this gives rise to the more familiar $M1$ transition operator

$$\mathbf{T}_{\mathrm{nr}} = -\frac{\sqrt{2}}{3} \frac{\omega}{c} \mu_0 (\mathbf{L} + 2\mathbf{S}). \tag{4}$$

where $\mathbf{L}$ and $\mathbf{S}$ are the orbital and spin angular momentum operators, respectively. In the LS-coupling scheme, which is realized in the nonrelativistic case, the $M1$ line strength is nonzero only between fine-structure levels with $\Delta J = \pm 1$. The reduced matrix element of $\mathbf{T}_{\mathrm{nr}}$ within the LS coupling is given

by

$$\langle J_f \parallel \mathbf{T}_{\mathrm{nr}} \parallel J_i \rangle = -\frac{\sqrt{2}}{3} \frac{\omega}{c} \mu_0 \langle J_f \parallel (\mathbf{J} + \mathbf{S}) \parallel J_i \rangle$$

$$= -\frac{\sqrt{2}}{3} \frac{\omega}{c} \mu_0 \langle J_f \parallel \mathbf{S} \parallel J_i \rangle,$$

which implies

$$S_{\mathrm{nr}} = |\langle J_f \parallel \mathbf{S} \parallel J_i \rangle|^2. \tag{5}$$

Therefore, in the nonrelativistic limit the line strength S_{nr} is completely determined by the quantum numbers of the initial and final states and does not depend on the radial part of the many-electron wave functions of the initial and final states. For the $^2P_{1/2} - {}^2P_{3/2}$ and $^2P_{3/2} - {}^2P_{1/2}$ fine-structure transitions, the nonrelativistic line strength results in the value of 4/3.

The total line strength can be calculated by adding different corrections to the nonrelativistic line strength as follows:

$$S = S_{\mathrm{nr}} + \Delta S_D + \Delta S_{\mathrm{CI,C}} + \Delta S_{\mathrm{CI,B}} + \Delta S_{\mathrm{QED}} + \Delta S_{\mathrm{rec}}. \tag{6}$$

Here ΔS_D is the correction due to the *relativistic* motion of the electrons as described by the (single-electron) Dirac equation. This correction is calculated as the difference between line strength evaluated between Eqs. (5) and (2). In Eq. (2) the initial- and final-state wave functions are linear combinations of Slater determinants constructed in terms of one-electron Dirac wave functions which are the solution of the noninteracting one-electron Dirac Hamiltonian

$$\hat{h}_D = c\boldsymbol{\alpha} \cdot \mathbf{p} + (\beta - 1)c^2 - V(r), \tag{7}$$

where V is the potential of a two-parameter Fermi nuclear charge distribution, β is the Dirac matrix, and c is the speed of light in atomic units.

The next two terms in Eq. (6) are due to the relativistic interelectronic interaction (correlations). While the first term $\Delta S_{\mathrm{CI,C}}$ arises from the Coulomb interaction, and the second $\Delta S_{\mathrm{CI,B}}$ occurs due to the Breit interaction. Both of these terms are evaluated in detail in Sec. II B. The next correction ΔS_{QED} originates from QED diagrams, namely, the self-energy diagrams. It is calculated here to all orders in αZ. The evaluation of this term is described in Sec. II C.

Finally, ΔS_{rec} is the correction to the line strength due to the finite nuclear mass effect. This effect can be calculated only by using a rigorous QED approach as described in Ref. [17]. According to this approach the recoil corrected magnetic moment operator is given by

$$\boldsymbol{\mu} = -\mu_0 \left(\mathbf{L} + 2\mathbf{S} - \frac{1}{M} \sum_{i,j} [\mathbf{r}_i \times \mathbf{p}_j] \right), \tag{8}$$

where M is mass of the nucleus. Hence the correction to the line strength due to the nuclear recoil can be written as

$$\Delta S_{\mathrm{rec}} \simeq -2\langle J_f \parallel (\mathbf{L} + 2\mathbf{S}) \parallel J_i \rangle$$

$$\times \left\langle J_f \parallel \frac{1}{M} \sum_{i,j} [\mathbf{r}_i \times \mathbf{p}_j] \parallel J_i \right\rangle. \tag{9}$$

However, these contributions are very small at the present level of accuracy compared to the leading nonrelativistic value 4/3. For example ΔS_{rec} amounts to 2.1×10^{-5}, 1.5×10^{-5},

0.9×10^{-5}, and 0.5×10^{-5} for B-like Ar, Fe, Mo, and W ions, respectively. Therefore, we do not present these values in our final table of the various contribution to line strengths.

B. Interelectronic-interaction corrections

To evaluate the interelectronic correlation correction arising due to Coulomb interaction $\Delta S_{CI,C}$, we apply systematically enlarged many-electron wave functions by using the latest version of the general purpose relativistic atomic structure package GRASP2K [23]. This package implements the multiconfiguration Dirac-Hartree-Fock (MCDHF) method in jj coupling [24]. In this method, Ψ is an atomic state function $\Psi(\Gamma; \pi J)$ for a state labelled Γ, where J is the total angular momentum quantum number and π is the parity. It is approximated by a linear combination of configuration state functions (CSFs) of the same symmetry:

$$\Psi(\Gamma; \pi J) = \sum_{j=1}^{n_c} c_j \Phi(\gamma_j; \pi J), \tag{10}$$

where n_c is the number of CSFs, c_j are the mixing coefficients, and γ_j denotes the orbital occupancy and angular coupling scheme of the jth CSF. The configuration state functions $\Phi(\gamma_j; \pi J)$ are a linear combination of Slater determinants of one electron Dirac spinors,

$$\Phi(r) = \frac{1}{r} \begin{pmatrix} P_{n\kappa}(r)\chi_\kappa^m(\theta,\varphi) \\ i\, Q_{n\kappa}(r)\chi_{-\kappa}^m(\theta,\varphi) \end{pmatrix}. \tag{11}$$

Here, κ is relativistic angular momentum quantum number, $P_{n\kappa}(r)$ and $Q_{n\kappa}(r)$ are the large and small radial components of the one-electron wave functions represented on a logarithmic grid, and χ_κ^m is the spinor spherical harmonic. The radial part of the Dirac orbitals and the expansion coefficients c_j are optimized to self-consistency from a set of equations which results from applying the variational principle on a weighted energy functional of the states in Dirac-Coulomb approximation [25] where the Dirac-Coulomb Hamiltonian $\hat{H}_{DC}$ is

$$\hat{H}_{DC} = \sum_{i=1}^{N}[c\boldsymbol{\alpha}_i \cdot \boldsymbol{p}_i + (\beta_i - 1)c^2 - V(r_i)] + \sum_{i<j}^{N} \frac{1}{r_{ij}}. \tag{12}$$

We first performed the calculations for the lowest-order approximation. For this the wave functions for the states with $J = 1/2$ and $J = 3/2$ are calculated within the basis of the multireference (MR) configurations. The CSFs in the MR set are generated from the configurations $\{1s^2 2s^2 2p, 1s^2 2p^3\}$, $\{1s^2 2s^2 2p^6 3s^2 3p, 1s^2 2s^2 2p^6 3p^3\}$, $1s^2 2s^2 2p^5$, and $1s^2 2s^2 2p^6 3s^2 3p^5$ for the B-, Al-, F-, and Cl-like ions, respectively. After the initial calculations, the wave functions are systematically improved by performing MCDHF calculations for each new layer of correlation orbitals and keeping the previous calculated orbitals fixed. For each new layer of correlation orbitals the basis of CSFs is expanded by including further single (S) and double (D) virtual excitations from the configurations defining the MR set to the active set of orbitals. The active set of orbitals is spanned by the orbitals with a principal quantum number $n \leqslant 7$ and with azimuthal quantum number $l \leqslant 6$. We also performed the calculations by including

TABLE I. Interelectronic-interaction correction ΔS_{CI} to the $M1$ line strength of the transition between the fine-structure levels of the ground configuration for B-, F-, Al-, and Cl-like Fe ions. The MCDHF and RCI methods are employed to evaluate these corrections considering Coulomb and Breit type interactions. They are presented as a function of the size of the increasing active set (AS) labeled by the highest principal quantum number n of the orbitals starting from the MR set.

AS	B-like Fe	F-like Fe	Al-like Fe	Cl-like Fe
MR	0.00053	0.00154	0.00149	0.00167
3	0.00052	0.00146	0.00148	0.00165
4	0.00049	0.00151	0.00146	0.00164
5	0.00050	0.00153	0.00145	0.00164
6	0.00045	0.00146	0.00147	0.00165
7	0.00045	0.00145	0.00147	0.00164

triple excitations from the MR set of orbitals. We found that the effect of triple excitation is of the order of 10^{-6} or smaller. This effect is negligible for the present level of accuracy.

Following each of the MCDHF calculations, separate relativistic configuration interaction (RCI) calculations are performed to further improve the initial- and final-state wave functions. These allowed us to evaluate the correction due to the Breit interaction $\Delta S_{CI,B}$ to the line strength. For these calculations the Dirac-Coulomb Breit Hamiltonian $\hat{H}_{DCB} = \hat{H}_{DC} + \hat{H}_{Breit}$ is used where

$$\hat{H}_{Breit} = -\sum_{i<j}^{N} \frac{1}{2r_{ij}} \left[\boldsymbol{\alpha}_i \cdot \boldsymbol{\alpha}_j + \frac{(\boldsymbol{\alpha}_i \cdot \boldsymbol{r}_{ij})(\boldsymbol{\alpha}_j \cdot \boldsymbol{r}_{ij})}{r_{ij}^2} \right]. \tag{13}$$

The sum of these two corrections gives rise to the total relativistic interelectronic-interaction correction ΔS_{CI}. These contributions are presented in Table I as a function of the size of the increasing active set labeled by the highest principal quantum number n of the of orbitals considered for the correlations. For the sake of brevity, we present the results only for the Fe ions. As seen from Table I, the convergence with regard to the size of the active set is fairly achieved, which allows us to set an absolute uncertainty for the interelectronic-interaction correction to a range of 1×10^{-5} to 5×10^{-5} depending on the particular ion.

C. QED correction

The QED correction to the $M1$ line strength ΔS_{QED} can be derived in lowest order in αZ by modifying the $M1$ transition operator of the atomic magnetic moment for the EAMM, as discussed in detail in Ref. [15]. The contribution of the EAMM amounts to $\Delta S_{QED,EAMM} = 0.00618$. In Ref. [16], moreover, the one-loop QED correction was calculated for several B-like ions to all orders in αZ within the so-called original Furry picture, and by taking into account only the Coulomb potential of the nucleus. We now consider an *extended* Furry picture which includes a local screening potential in the unperturbed Hamiltonian, and extends the calculations for F-, Al-, and Cl-like systems. This extension enables us to partially account for the screening QED corrections by evaluating only one-electron QED diagrams. In the extended Furry picture,

we solve the Dirac equation with an effective spherically symmetric potential treating the interaction with the external Coulomb potential of the nucleus and the local screening potential exact to all orders. We employ here the core-Hartree screening potential, which is given by the expression

$$V_{scr}(r) = \int_0^\infty dr' \frac{1}{r_>} \rho_{core}(r').$$ (14)

Here ρ_{core} denotes the total radial charge density distribution of the core electrons

$$\rho_{core}(r) = \sum_c \left[P_c^2(r) + Q_c^2(r) \right],$$

$$\int_0^\infty dr \rho_{core}(r) = n_c,$$ (15)

where n_c is the number of the core electrons, i.e., $n_c = 4, 8, 12, 16$ for B-, F-, Al-, and Cl-like ions, respectively. This screening potential is generated self-consistently by solving the Dirac equation until the energies of the core and valence states become stable with the relative accuracy of 10^{-9}. To estimate the sensitivity of the result on the choice of the potential, several tests have been performed with other screening potentials: Kohn-Sham, Dirac-Hartree, and Dirac-Slater constructed for the initial as well as for the final state. It has been found out that a relative difference between results obtained with different potentials does not exceed 5×10^{-4}. Overall, therefore, the uncertainty is dominated by a numerical error, which is everywhere smaller than 10^{-5}.

The one-loop QED correction to the line strength consists of the self-energy and vacuum-polarization terms. However, the vacuum-polarization correction previously evaluated in the Uehling approximation appears to be two to four orders of magnitude smaller than the self-energy correction beyond the EAMM approximation [26]. For this reason, we neglect the vacuum-polarization term in the present consideration. The self-energy contribution is given by the diagrams depicted in Fig. 1. While the formulas derived in Ref. [16] in the original Furry picture remain formally the same, let us recall that the Dirac spectrum is now generated by solving the Dirac equation with the effective potential. We make use of the implementation

of Ref. [16] where a detailed description of these calculations for B-like ions is presented.

III. RESULTS AND DISCUSSION

Table II lists different corrections to the nonrelativistic line strength for the $M1$ transition between the fine-structure levels of the ground configurations in B-like and F-like Ar, Fe, Mo, and W ions. These corrections refer to two different systems of p subshells, one with a single valence electron and the other with a single vacancy in the L shell. Table III shows similar results as Table II but for the M shell for Al-like and Cl-like Fe, Mo, and W ions. As seen from Tables II and III the relativistic correction ΔS_D is most important. Its value increases by an order of magnitude for the Mo and W ions when compared to Ar and Fe ions. The interelectronic-interaction correction arising due to the Breit interaction turns out to be relatively small as compared to corrections arising due to the Coulomb interaction. For Mo and W ions these corrections

TABLE II. Individual corrections to the $M1$ nonrelativistic line strength $S_{nr} = 4/3$ for the $(2s^2 2p)\,^2P_{1/2} - {}^2P_{3/2}$ transition in B-like as well as for the $(2s^2 2p^5)\,^2P_{3/2} - {}^2P_{1/2}$ transitions in F-like Ar, Fe, Mo, and W ions. The total line strength (S) is compared with other theories. The uncertainties involved in the calculation of line strengths are given within the parentheses.

	Ar	Fe	Mo	W
B-like				
ΔS_D	−0.00295	−0.00633	−0.01800	−0.07402
$\Delta S_{CI,C}$	0.00056	0.00038	−0.00247	−0.00530
$\Delta S_{CI,B}$	0.00001	0.00007	0.00042	0.00166
ΔS_{QED}	0.00617	0.00615	0.00606	0.00567
S	1.33714(28)	1.33362(23)	1.3194(10)	1.2614(18)
	1.3372[a]	1.3337[a]	1.3197[a]	
	1.33693(26)[b]	1.333[c]*		
	1.337[c]*	1.333[d]*		
	1.337[d]*			
F-like				
ΔS_D	−0.00295	−0.00633	−0.01800	−0.07402
$\Delta S_{CI,C}$	0.00094	0.00143	0.00258	0.00569
$\Delta S_{CI,B}$	0.00000	0.00002	0.00006	0.00036
ΔS_{QED}	0.00617	0.00615	0.00607	0.00568
S	1.33749(47)	1.33460(70)	1.3240(13)	1.2710(30)
	1.356(5)[e]*	1.335[g]*	1.324[h]*	1.271[f]*
	1.338[f]*	1.334[f]*	1.324[f]*	1.271[i]*
		1.3270[j]*	1.3211[j]*	

[a]MCDHF theory by Froese Fischer *et al.* [20].
[b]MC-DFS theory by Tupitsyn *et al.* [15].
[c]MCDF theory by Rynkun *et al.* [18].
[d]MCDF theory by Marques *et al.* [19].
[e]Relativistic coupled-cluster theory by Nandy [27].
[f]MCDF theory by Jönsson *et al.* [28].
[g]MCDF theory by Jonauskas *et al.* [29].
[h]MCDF theory by Aggarwal and Keenan [30].
[i]MCDF theory by Aggarwal and Keenan [31].
[j]Relatively coupled-cluster theory by Nandy and Sahoo [32].
*The original values are corrected by adding the QED correction obtained here.
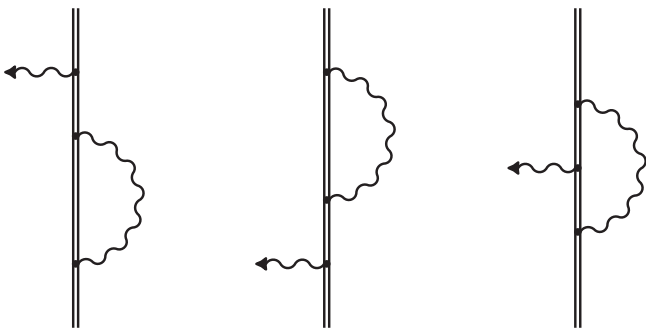

FIG. 1. Feynman diagrams that represent the self-energy correction to the line strength. The wavy line indicates the photon propagator and the double line indicates the bound-electron wave functions and propagators in the effective potential being the sum of Coulomb and screening potentials. The single-photon emission is depicted by the wavy line with arrow.

TABLE III. Individual corrections to the $M1$ nonrelativistic line strength $S_{nr} = 4/3$ for the $(3s^2 3p)\,^2P_{1/2} - \,^2P_{3/2}$ transition in Al-like as well as for the $(3s^2 3p^5)\,^2P_{3/2} - \,^2P_{1/2}$ transition in Cl-like Fe, Mo, and W ions. The total line strength (S) is compared with other theories. The uncertainties involved in the calculation of line strengths are given within the parentheses.

	Fe	Mo	W
Al-like			
ΔS_D	−0.00302	−0.00950	−0.05025
$\Delta S_{CI,C}$	0.00146	0.00230	0.00340
$\Delta S_{CI,B}$	0.00001	0.00007	0.00054
ΔS_{QED}	0.00617	0.00614	0.00595
S	1.33797(73)	1.3324(13)	1.2928(20)
	1.336[a]*		
	1.337[b]		
Cl-like			
ΔS_D	−0.00302	−0.00950	−0.05025
$\Delta S_{CI,C}$	0.00164	0.00294	0.00615
$\Delta S_{CI,B}$	0.00000	0.00005	0.00029
ΔS_{QED}	0.00617	0.00614	0.00595
S	1.3381(18)	1.3330(15)	1.2955(32)
	1.338[c]*		1.295[d]*
	1.338[e]		1.29[f]*

[a]MR-MP theory by Vilkas and Ishikawa [21].
[b]MR-MP theory by Santana et al. [22].
[c]B-spline single-particle orbitals method by Moehs et al. [33].
[d]MCDF method by Aggarwal and Keenan [34].
[e]MR-MP theory by Ishikawa et al. [35].
[f]MCDF theory by Singh and Puri [36].
*The original values are corrected by adding the QED correction obtained here.

provide essential contributions to the total line strengths. The next important correction arises from the self-energy (QED). Generally, the lowest order QED correction, i.e., the inclusion of EAMM to the transition operator, is considered enough for such transitions. As discussed in Sec. II C this correction amounts to 0.00618 the total line strength. However, the present estimates of the QED correction show that the inclusion of the EAMM is enough only for low Z. For the heavier systems the present rigorous calculations of QED corrections within an extended Furry picture approach are necessary. Finally, all corrections sum to the total line strength S. To estimate the total uncertainty we have to note here that the contribution of the negative-energy excitations is not taken into account in the present calculations. Since the value of the negative-continuum term strongly depends on the employed one-electron basis functions [15], by varying them we estimate its contribution to be less than half of the correlation effect. The uncertainties of individual terms presented in Tables II and III as discussed above in corresponding sections are much smaller than the uncertainty due to the negative-continuum contribution. Therefore, the total uncertainty of the line strength S obtained is fully determined by the missing negative-continuum contribution.

To compare our results with previous computations, we make use of the line strength from $M1$ transition rates based on Eq. (1). We take the same transition energies that were used in respective calculations. It should be noted that we

have added the QED contribution to the line strengths in respective theoretical values wherever this effect has not been considered. For B-like Ar, which has received much attention over the last decade, our result of total line strength 1.33714(28) corroborates the two exceptionally agreeing calculations from Tupitsyn et al. [15] and Fischer et al. [20]. Tupitsyn et al. [15] reported the line strength value 1.33693(26) for B-like Ar. Additionally, Fischer et al. [20] reported a line strength 1.3372 for B-like Ar. Fischer et al. [20] further extended their calculations for the B-like isoelectronic sequence until $Z = 42$. As seen from Table II our results also agree with B-like Fe and B-like Mo. Our results of the line strengths for all other systems under present study are in agreement with other available theories. The only exception is with the relativistic coupled-cluster calculations for which the line strength of 1.356(5) in F-like Ar of Ref. [27] is overestimated and the line strength of 1.3270 in F-like Fe of Ref. [32] is underestimated. This may be due to the incorrect handling of intruder states in the implementation of coupled-cluster theory in open-shell systems [37]. Overall, our calculations have reached an accuracy of $10^{-4} - 10^{-5}$ for the QED sensitive $M1$ line strengths between the fine-structure levels of the same configuration. As a result, the present calculations provide a theoretical prerequisite for a test of QED effects in the line strengths of various ions.

In Table IV we present the lifetimes τ_{pres} (in seconds) calculated for the $(2s^2 2p)\,^2P_{3/2}$ level in B-like ions, the $(2s^2 2p^5)\,^2P_{1/2}$ level in F-like ions, the $(3s^2 3p)\,^2P_{3/2}$ level in Al-like ions as well as for the $(3s^2 3p^5)\,^2P_{1/2}$ level in Cl-like ions. Here, τ_{expt} are experimental lifetimes and the respective experimental uncertainties are given in parentheses. A_{M1} is the present transition rate from the $M1$ channel. We used the best available transition energies from the literature for the calculation of the transition rate. For B-like ions we applied the transition energies from the rigorous QED treatment of Artemyev et al. [2,4], and for the rest of the ions we used transition energies from the NIST database [38]. Here A_{E2} is the transition rate from the $E2$ channel in length form. For the $E2$ transition rate, we use same wave-function expansion as for the $M1$ transition rate; in addition to that, the length and the velocity gauges of the $E2$ line strength were in good agreement. Let us note that the present uncertainties in transition rates and lifetimes are due to uncertainties in the calculation of the $M1$ line strengths only. They are given within the parentheses. For the present level of accuracy, the uncertainties due to the $E2$ transition channel are very small. However, the uncertainties in the transition energies will increase total uncertainties in our calculations accordingly.

As seen from Table IV, our predicted lifetimes for B-like Ar and for Al-like Fe disagree with both experiments at the HD-EBIT [13,14]. In contrast, the comparison of our predicted lifetime for F-like Ar with the experiment at the LLNL-EBIT [8] and for the lifetime of Cl-like Fe with the experiment at the HD-EBIT [39] shows very good agreement. For Cl-like Fe, our lifetime also agrees well with the extrapolated lifetime of Ref. [40] which is resulted in an experimental study along Cl-like Co, Ni, and Cu ions. These experiments with an uncertainty larger than 0.5% are not, however, sensitive enough to test the underlying relativistic correlations and the leading QED effects. New experiments with the soft x-ray free electron

TABLE IV. Lifetimes τ_{pres} (in seconds) calculated for the $(2s^2 2p)\ ^2P_{3/2}$ level in B-like ions, the $(2s^2 2p^5)\ ^2P_{1/2}$ level in F-like ions, the $(3s^2 3p)\ ^2P_{3/2}$ level in Al-like ions, and the $(3s^2 3p^5)\ ^2P_{1/2}$ level in Cl-like ions compared with experimental lifetimes (τ_{expt}). A_{M1} is the present transition rate (in s^{-1}) from the $M1$ channel and A_{E2} is the transition rate (in s^{-1}) from the $E2$ channel. The values of the transition energy used for the present lifetime calculations are given in cm^{-1} and corresponding transition wavelengths λ in Å. The uncertainties involved in the calculation of transition rate and lifetime arising due to uncertainties in the line strengths are given within the parentheses. The numbers given in the square brackets denote powers of 10.

Ions	Energy	λ	A_{M1}	A_{E2}	τ_{pres}	τ_{expt}
B-like						
Ar^{13+}	22656.92	4413.663	1.0487(02)[+02]	1.86[−03]	9.5354(20)[−03]	9.573(4)(5)[−03][a]
						8.7(5)[−03][b]
						9.12(18)[−03][c]
						9.70(15)[−03][d]
Fe^{21+}	118310.243	845.235	1.4893(03)[+04]	1.37[+00]	6.7141(11)[−05]	
Mo^{37+}	964437.459	103.687	7.9810(60)[+06]	6.00[+03]	1.2520(09)[−07]	
W^{69+}	11802649.713	8.473	1.3985(20)[+10]	1.25[+08]	7.0874(10)[−11]	
Al-like						
Fe^{13+}	18852.5	5304.336	6.0455(33)[+01]	1.49[−02]	1.6537(09)[−02]	1.6726(+20/-10)[−02][e]
						1.7(2)[−02][f]
						1.674(12)[−02][g]
						1.752(29)[−02][h]
Mo^{29+}	204020	490.148	7.6299(74)[+04]	1.67[+02]	1.3078(12)[−05]	
W^{61+}	2933400	34.090	2.2008(34)[+08]	6.30[+06]	4.4174(70)[−09]	
F-like						
Ar^{9+}	18067.494	5534.802	1.0639(04)[+02]	2.11[−03]	9.3994(33)[−03]	9.32(12)[−03][d]
Fe^{17+}	102579	974.858	1.9428(10)[+04]	1.94[+00]	5.1466(26)[−05]	
Mo^{33+}	886305	112.828	1.2432(12)[+07]	9.77[+03]	8.0372(79)[−08]	
W^{65+}	11202000	8.927	2.4097(57)[+10]	2.16[+08]	4.1131(98)[−11]	
Cl-like						
Fe^{9+}	15683.14	6376.274	6.9615(93)[+01]	1.52[−02]	1.4362(19)[−02]	1.42(2)[−02][i]
						1.441(14)[−02][j]
						1.364(25)[−02][h]
Mo^{25+}	186950	534.902	1.1746(13)[+05]	2.41[+02]	8.4959(96)[−06]	
W^{57+}	2796000	35.765	3.8190(94)[+08]	1.05[+07]	2.5485(65)[−09]	

[a]HD-EBIT experiment by Lapierre *et al.* [13].
[b]NIST-EBIT experiment by Serpa *et al.* [6].
[c]ECRIS in a Kingdon ion trap experiment by Moehs *et al.* [5].
[d]LLNL-EBIT by Träbert *et al.* [8].
[e]HD-EBIT experiment by Brenner *et al.* [14].
[f]ECRIS in a Kingdon ion trap experiment by Smith *et al.* [10].
[g]LLNL-EBIT experiment by Beiersdorfer *et al.* [9].
[h]ECRIS in a Kingdon ion trap by Moehs and Church [7].
[i]HD-EBIT experiment by Brenner *et al.* [39].
[j]TSR measurements at the Max Planck Institute for Nuclear Physics, Heidelberg, Germany by Träbert *et al.* [40].

laser (FLASH) and a new EBIT [41] along with the pump probe x-ray laser experiments [42] will hopefully provide experimental data for the transitions with short lifetimes in so far inaccessible energy ranges. We believe that our calculations will support such future experiments for transitions with different frequencies and lifetimes.

IV. CONCLUSION

In this paper, we have presented highly accurate calculations for the line strengths of QED-sensitive forbidden transitions by utilizing the multiconfiguration Dirac-Hartree-Fock and relativistic configuration interaction methods. We have ex-

tended the high-precision evaluations previously performed for the middle Z B-like ions [15,20] to higher Z as well as to different systems such as F-, Al-, and Cl-like ions. In our systematically enlarged wave functions, we incorporated all important electron correlations and the effects of relativity by taking the Coulomb and Breit interactions into account. The obtained line strengths are further improved by rigorous calculations of the QED correction within an extended Furry picture approach. We used up-to-date accurate transition energies for the calculations of the $M1$ transition rates and reported lifetimes in the millisecond to picosecond range. We believe that our accurate theoretical predictions provide the prerequisite for a test of QED by lifetime measurements

at different frequencies and timescales. This will help to find a reason for the present discrepancies between theory and experiment for B-like Ar and Al-like Fe. Apart from testing atomic structure theory, such experiments in the future agreeing with the theoretical investigations will be very helpful for terrestrial and astrophysical plasma diagnostics.

[1] I. Draganić, J. R. Crespo López-Urrutia, R. DuBois, S. Fritzsche, V. M. Shabaev, R. S. Orts, I. I. Tupitsyn, Y. Zou, and J. Ullrich, Phys. Rev. Lett. **91**, 183001 (2003).

[2] A. N. Artemyev, V. M. Shabaev, I. I. Tupitsyn, G. Plunien, and V. A. Yerokhin, Phys. Rev. Lett. **98**, 173004 (2007).

[3] V. Mäckel, R. Klawitter, G. Brenner, J. R. Crespo López-Urrutia, and J. Ullrich, Phys. Rev. Lett. **107**, 143002 (2011).

[4] A. N. Artemyev, V. M. Shabaev, I. I. Tupitsyn, G. Plunien, A. Surzhykov, and S. Fritzsche, Phys. Rev. A **88**, 032518 (2013).

[5] D. P. Moehs and D. A. Church, Phys. Rev. A **58**, 1111 (1998).

[6] F. G. Serpa, J. D. Gillaspy, and E. Träbert, J. Phys. B **31**, 3345 (1998).

[7] D. P. Moehs and D. A. Church, Astrophys. J. **516**, L111 (1999).

[8] E. Träbert, P. Beiersdorfer, S. B. Utter, G. V. Brown, H. Chen, C. L. Harris, P. A. Neill, D. W. Savin, and A. J. Smith, Astrophys. J. **541**, 506 (2000).

[9] P. Beiersdorfer, E. Träbert, and E. H. Pinnington, Astrophys. J. **587**, 836 (2003).

[10] S. J. Smith, A. Chutjian, and J. A. Lozano, Phys. Rev. A **72**, 062504 (2005).

[11] E. Träbert, Can. J. Phys. **86**, 73 (2008).

[12] E. Träbert, Atoms **2**, 15 (2014).

[13] A. Lapierre, U. D. Jentschura, J. R. Crespo López-Urrutia, J. Braun, G. Brenner, H. Bruhns, D. Fischer, A. J. González Martínez, Z. Harman, W. R. Johnson, C. H. Keitel, V. Mironov, C. J. Osborne, G. Sikler, R. Soria Orts, V. Shavaev, H. Tawara, I. I. Tupitsyn, J. Ullrich, and A. Volotka, Phys. Rev. Lett. **95**, 183001 (2005).

[14] G. Brenner, J. R. Crespo López-Urrutia, Z. Harman, P. H. Mokler, and J. Ullrich, Phys. Rev. A **75**, 032504 (2007).

[15] I. I. Tupitsyn, A. V. Volotka, D. A. Glazov, V. M. Shabaev, G. Plunien, J. R. Crespo López-Urrutia, A. Lapierre, and J. Ullrich, Phys. Rev. A **72**, 062503 (2005).

[16] A. V. Volotka, D. A. Glazov, G. Plunien, V. M. Shabaev, and I. I. Tupitsyn, Eur. Phys. J. D **38**, 293 (2006).

[17] A. V. Volotka, D. A. Glazov, G. Plunien, V. M. Shabaev, and I. I. Tupitsyn, Eur. Phys. J. D **48**, 167 (2008).

[18] P. Rynkun, P. Jönsson, and G. Gaigalas, and C. F. Fischer, At. Data Nucl. Data Tables **98**, 481 (2012).

[19] J. P. Marques, P. Indelicato, and F. Parente, Eur. Phys. J. D **66**, 324 (2012).

[20] C. F. Fischer, I. P. Grant, G. Gaigalas, and P. Rynkun, Phys. Rev. A **93**, 022505 (2016).

[21] M. J. Vilkas and Y. Ishikawa, Phys. Rev. A **68**, 012503 (2003).

[22] J. A. Santana, Y. Ishikawa, and E. Träbert, Phys. Scr. **79**, 065301 (2009).

[23] P. Jönsson, G. Gaigalas, J. Bieroń, C. Froese Fischer, and I. P. Grant, Comput. Phys. Commun. **184**, 2197 (2013).

[24] I. P. Grant, *Relativistic Quantum Theory of Atoms and Molecules*, (Springer, New York, 2007).

[25] K. G. Dyall, I. P. Grant, C. T. Johnson, F. A. Parpia, and E. P. Plummer, Comput. Phys. Commun. **55**, 425 (1989).

[26] A. V. Volotka, Ph.D. thesis, Technische Universität Dresden, 2006.

[27] D. K. Nandy, Phys. Rev. A **94**, 052507 (2016).

[28] P. Jönsson, A. Alkauskas, and G. Gaigalas, At. Data Nucl. Data Tables **99**, 431 (2013).

[29] V. Jonauskas, F. P. Keenan, M. E. Foord, R. F. Heeter, S. J. Rose, P. A. M. van Hoof, G. J. Ferland, K. M. Aggarwal, R. Kisielius, and P. H. Norrington, Astron. Astrophys. **416**, 383 (2004).

[30] K. M. Aggarwal and F. P. Keenan, At. Data Nucl. Data Tables **109-110**, 205 (2016).

[31] K. M. Aggarwal and F. P. Keenan, At. Data Nucl. Data Tables **111-112**, 187 (2016).

[32] D. K. Nandy and B. K. Sahoo, Astron. Astrophys. **563**, A25 (2014).

[33] D. P. Moehs, M. I. Bhatti, and D. A. Church, Phys. Rev. A **63**, 032515 (2001).

[34] K. M. Aggarwal and F. P. Keenan, At. Data Nucl. Data Tables **100**, 1603 (2014).

[35] Y. Ishikawa, J. A. Santana, and E. Träbert, J. Phys. B **43**, 074022 (2010).

[36] G. Singh and N. K. Puri, J. Phys. B **49**, 205002 (2016).

[37] H. Gharibnejad and A. Derevianko, Phys. Rev. A **86**, 022505 (2012).

[38] A. Kramida, Yu. Ralchenko, J. Reader, and NIST ASD Team, NIST Atomic Spectra Database (ver. 5.5.2) (2018). Available: http://physics.nist.gov/asd

[39] G. Brenner, J. R. Crespo López-Urrutia, S. Bernitt, D. Fischer, R. Ginzel, K. Kubiček, V. Mäckel, P. H. Mokler, M. C. Simon, and J. Ullrich, Astrophys. J. **703**, 68 (2009).

[40] E. Träbert, G. Saathoff, and A. Wolf, J. Phys. B **37**, 945 (2004).

[41] S. W. Epp, Phys. Rev. Lett. **98**, 183001 (2007).

[42] E. Träbert, Appl. Phys. B **114**, 167 (2014).